33rd Annual International Conference of the IEEE EMBS
Boston, Massachusetts USA, August 30 - September 3, 2011

Detecting the Pigment Network in Dermoscopy Images: a Directional Approach

Catarina Barata   Jorge S. Marques   Jorge Rozeira

***Abstract*— Several algorithms have been recently proposed for the analysis of dermoscopy images and the detection of melanomas. However, the pigment network is not considered in most of these works, although this cue plays a major role in clinical diagnosis routines. This paper proposes an algorithm for the detection of the pigment network. The algorithm is based on a bank of directional filters (difference of Gaussians) and explores color, directionality and topological properties of the network.**

I. Introduction

Dermoscopy is a non-invasive diagnosis tool for the analysis of skin lesions, allowing an early detection of melanomas. The lesion is covered with gel and observed through an optical system (dermatoscope) which magnifies the lesion by a factor of 6x to 80x [1]. This procedure significantly improves the diagnosis accuracy. Systematic studies have proved that in melanoma diagnosis, an increase of sensitivity of $10 - 27\%$ is observed when dermatoscopy images are available [2].

Several methods have been proposed by clinicians for the classification of malignant lesions using dermoscopy images. Some notable examples are the Pattern Analysis [3], Menzies method [4], ABCD rule [5] and 7 point checklist [6]. In all these methods the expert is asked to identify structures, colors and symmetry in the skin lesions. This requires a long training and the decision is subjective since similar cues may be present in different types of lesions.

The importance of skin cancer detection and the complexity of the decision fostered the development of algorithms for the analysis of skin lesions and melanoma detection. Most of these algorithms perform an automatic segmentation of the lesion and compute a large number of features: shape, color and texture features [7], [8], [9]. Learning algorithms are then used to select the most useful features and to provide a binary decision (malignant or not). Very promising results have been obtained in some of these approaches and there is currently one automatic system available on the net [8].

The above methods adopt a statistical approach and do not try to incorporate detailed medical knowledge. They are based on the machine learning paradigm: if features are rich enough and if we have a (very) large database of lesions, inference methods (SVM, neural networks, boosting) will be able to learn the classification rule [10]. A different approach has been used by other authors who try to detect the medical features used by dermatologists (e.g., symmetry, specific colors, differential structures such as streaks, dots or vascular networks) [11], [12], [13], [14], [15].

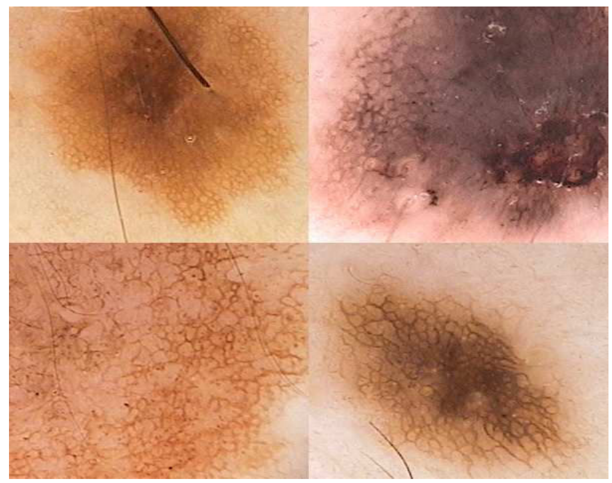

Fig. 1. Pigment network in dermoscopy images

However, most of these systems do not extract the pigment network which is considered a key structure in dermoscopy (see Fig. 1). For example it is a fundamental cue to discriminate melanocytic lesions from non-melanocytic ones. The presence or absence of this network and its properties (line width (thin or thick), the spatial organization (regular or irregular)) are important cues for the classification of pigmented lesions. Unfortunately, this issue has not been addressed in the literature with few notable exceptions [11], [14]. In fact, this is challenging problem since it is difficult to reliably detect the pigment network and discriminate it from other structures present in the skin and lesion.

This paper addresses the detection of the pigment network using a bank of directional filters, followed by a topological analysis of the detected regions. The paper is organized as follows. Section 2 presents an overview of the proposed system. Section 3 describes the filter bank. Section 4 and 5 present pre-processing and network detection algorithms. Section 6 describes an experimental evaluation of the methods and section 7 concludes the paper.

II. System Overview

The pigment network is a subtle color pattern which appears in many skin lesions and plays an important role in medical diagnosis. This pattern is produced by the presence of melanocytes or melanin cells under the outer layer of the

This work was supported by FCT in the scope of project PTDC/SAU-BEB/103471/2008

C. Barata and J. S. Marques are with Institute for Systems and Robotics, Instituto Superior Tecnico, Portugal `jsm@isr.ist.utl.pt`

J. Rozeira is with the Hospital Pedro Hispano, Matosinhos, Portugal.

skin and may exhibit different visual properties, namely different color, width and spatial organization. Some examples are shown in Fig. 1.

Despite this variability, some visual properties can be used to detect the network and discriminate it from other structures such as blobs. Two properties will be considered: *i) color:* the network consists of a set of brown lines superimposed on a lighter background; and *ii) spatial organization:* the lines form a connected net with holes of lighter color. The holes tend to have an hexagonal shape and may exhibit a quasi-periodic distribution in space.

In practice, there are additional difficulties. dermoscopy images often have multiple artifacts due to the presence of hairs or reflections produced during the acquisition process. These artifacts have to be removed or attenuated before we try to detect the network.

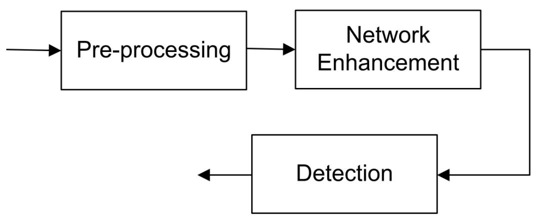

Fig. 2. Block diagram of the detection system

The detection system described in this paper consists of three main blocks (see Fig. 2): *i) pre-processing ii) network enhancement and iii) network detection*. The first block detects artifacts and removes them from the image; the second block emphasizes the network structure taking into account its color and spatial properties, while the third block detects the presence of the pigment network using this information.

III. Directional Filters

The pigment network and some of the artifacts (hairs) contain linear strokes. Therefore, we will adopt directional filters to enhance such structures. Since we do not know the stokes directions, we will use several directional filters each of them tuned to a specific orientation $\theta_i \in [-\pi/2, \pi/2[$, $i = 1, \ldots, N$. The output of the directional filter is then compared with the output of an omni directional filter. We will use Gaussian filters for this purpose.

Considering both contributions, the filter impulse response is given by

$$h_\theta(x,y) = G_1(x,y) - G_2(x,y) \tag{1}$$

where $G_k(x,y)$ is a Gaussian filter

$$G_k(x,y) = C_k \exp\left\{ -\frac{x'^2}{2\sigma^2_{x,k}} - \frac{y'^2}{2\sigma^2_{y,k}} \right\} \quad k = 1,2 \tag{2}$$

C_k is a normalization constant and (x', y') are related to (x, y) by a rotation of amplitude θ

$$x' = x\cos\theta + y\sin\theta \tag{3}$$

$$y' = -x\sin\theta + y\cos\theta \tag{4}$$

The filter parameters $\sigma^2_{x,k}, \sigma^2_{y,k}$ are chosen in such a way that the second filter is highly directional and the first is less directional or even isotropic.

We filter a gray level image I using all directional filters

$$I_i(x,y) = h_{\theta_i}(x,y) * I(x,y) \tag{5}$$

The outputs of the directional filters I_i are then combined as follows. We select the maximum output at each pixel

$$J(x,y) = \max_i I_i(x,y) \tag{6}$$

IV. Pre-Processing

Let us describe the first processing step in this algorithm: pre-processing. This block performs two key operations: hair detection and reflection detection. First we convert the dermoscopic image (RGB image) into a gray scale image. We choose one of the color channels (the one with highest entropy). Then we apply the procedures described below.

Hair detection

This block tries to detect hair pixels in the gray level image. Hairs are long, linear and dark structures. We filter the gray scale image I using a bank of directional filters (1-6). If the filters response $J(x,y)$ exceeds a threshold T_h the pixel (x,y) is classified as hair.

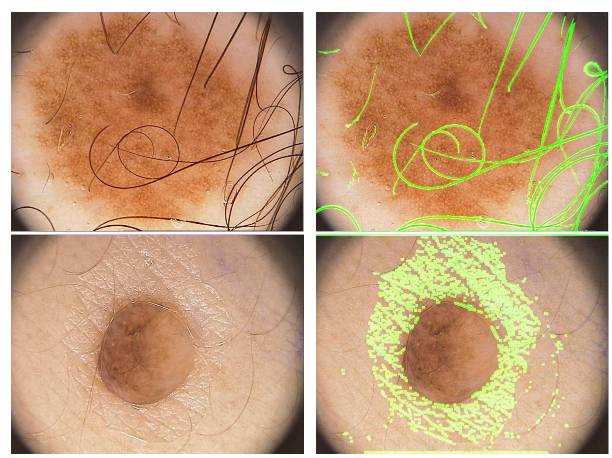

Fig. 3. Detection of hair (1st row) and reflections (2nd row).

Reflection detection

The reflection detection algorithm is very simple. We classify a pixel (x,y) as reflection if its intensity is high and if it is higher than the average intensity $I_{av}(x,y)$ computed in a neighborhood of the pixel. Therefore, the pixel should meet the following condition

$$I(x,y) > T_{r1} \quad \wedge \quad I(x,y) - I_{av}(x,y) > T_{r2} \tag{7}$$

where T_{r1}, T_{r2} are thresholds and I_{av} is the average intensity. Figure 3 shows examples of both pre-processing operations.

Image Inpainting

We remove the artifacts (reflections, hairs) detected in the previous step by multiplying the gray level image by a binary mask obtained in previous steps (hair and reflection detection). We then use an interpolation (inpainting) algorithm to fill the gaps. This algorithm is used to fill the gaps and interpolate the image in unknown regions, using known image pixels (context information) [16]. This reduces the influence of artifacts and avoids false alarms i.e., the detection of features which do not exist.

V. NETWORK DETECTION

The pigment network is a grid of lines which can be observed inside the lesion. The key question is: *what distinctive features can be used to separate the network from other structures of the skin?* At least two features can be used. The color of the lines (thin dark lines over a lighter background) and their spatial organization. These features (color and geometry) will be explored in the automatic network detection algorithm.

We proceed as follows. First we apply a bank of directional filters to detect the dark lines, using difference of Gaussians (see (1-6)). These filters are similar to the ones used for the hair detection. However the filter parameters are different since the length of each line stroke in the pigment network is much smaller than the case of the hairs. The output of the filter bank is then combined with the binary masks obtained in the previous steps (pre-processing) in order to discard the artifacts.

The second step is based on geometry. We assume that the pigment network is connected. Therefore, we extract all the connected components in the binary image obtained in the first step and extract all the connected regions whose area is larger than a threshold. Let R_i denote the $i-th$ connected region. We enforce the following condition

$$A(R_i) > A_{min} \tag{8}$$

where $A(R_i)$ denotes the area of R_i and A_{min} is the threshold which was experimentally found. This step discards all the connected components with a small area. The pigment network region is the union of all connected components meeting condition (8)

$$R = \bigcup_{i:A(R_i)>T_n} R_i \ . \tag{9}$$

VI. RESULTS

The algorithm described in previous sections was tested on a set of 55 dermoscopic images, extracted from the database of Hospital Pedro Hispano, Matosinhos, 13 of these images have pigment network; the others do not have this network or it is not visible in the image. This set contains RGB images of size 576×767, stored in *bitmap* and *jpeg* formats. Each color component is in the range $0, \ldots, 255$. The images were acquired during clinical exams using a dermatoscope and a magnification of $20\times$.

The algorithm was applied using the same parameters for all the images in the data set. Hair detection: $N =$ 64 filters, $\sigma_{x,1} = 20, \sigma_{y,1} = 6, \sigma_{x,2} = 20, \sigma_{y,2} = 0.5$ pixels, $T_h = 0.06$, filter mask 41×41; reflections detection: $T_{r1} = 180, T_{r2} = 25$,; network detection: $N = 18$ filters, $\sigma_{x,1} = 40, \sigma_{y,1} = 40, \sigma_{x,2} = 3, \sigma_{y,2} = 0.5$ pixels, $T_h = 0.0185, A_{min} = 700$ pixels, filter mask 11×11.

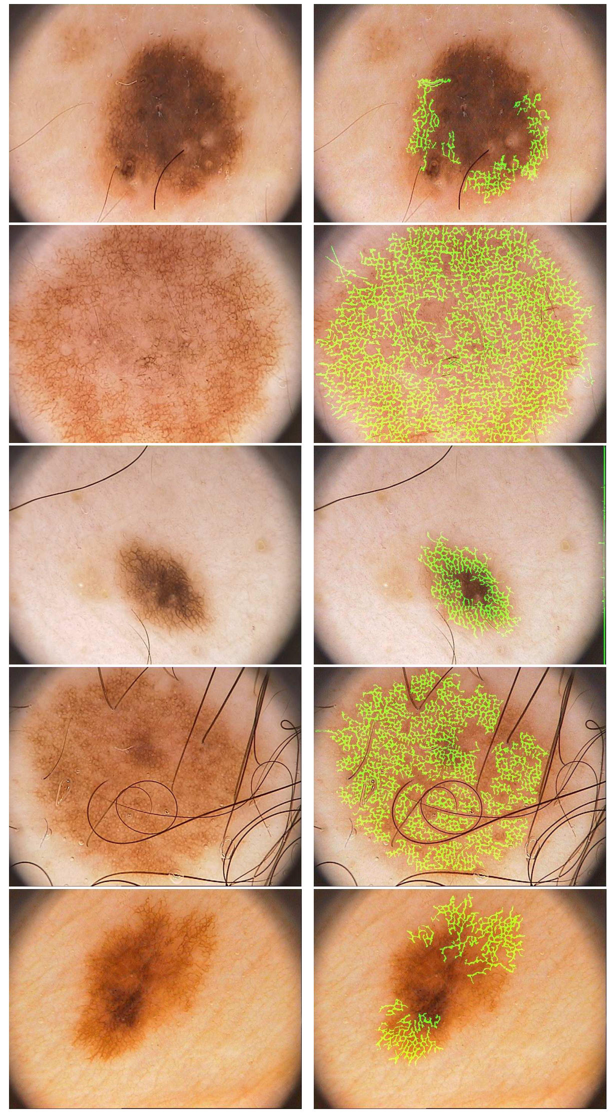

Fig. 4. Detection of pigment network: original images (left) and pigmented network (right)

The algorithm was applied to the set of 55 images. Figure 4 shows several examples in which the network was detected by the algorithm. On the left column we show the original images and on the right the detected network. The algorithm manages to detect the pigment network well in all these examples despite the fact that the pattern is rather subtle in some of them.

Next we show some examples in which the detector fails. Figure 5 shows two lesions with a strong texture with large and dark circular structures. This texture is detected although it is not a pigment network. In this case, the algorithm detects the boundaries of the circular structures which form a connected component.

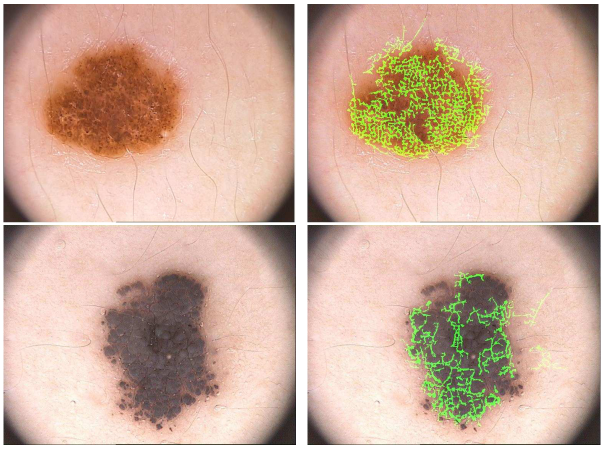

Fig. 5. Detection errors: original images (left) and pigmented network (right)

	not detected	detected
no network	67.5%	32.5%
pigment network	20,0%	80.0%

TABLE I

STATISTICAL RESULTS

It is useful to perform a binary classification of the images according to the presence of the pigment network. To improve the results, the network detected by the previous algorithm should be verified to check if it has the expected properties, e.g., pigment color, background color, statistics of holes and spatial organization of holes. An automatic classifier can be trained from this data to learn the decision and improve the results obtained by thresholding. In this paper, we take a simpler approach. We compare the network area with a threshold and use this test to classify the image into one of two classes: *with* and *without pigment network*. The threshold is chosen as 10% of the lesion area. Table 1 shows the results obtained using this simple test in the data set of 55 images.

The algorithm obtained a specificity SP=67.5% and a sensibility SE=80.0% in this data set of clinical examples.

These statistics describe the output of the algorithm without any additional post-processing to verify if the detected networks are correct.

VII. CONCLUSION

This paper presents an algorithm for the detection of the pigment network. The proposed algorithm explores the line color and geometry as well as the network topology using a bank of directional filters. Experimental results in a set of annotated images from Hospital Pedro Hispano show that the algorithm achieves good detection scores and it is therefore an useful tool in a dermoscopy analysis system.

Future work should focus on a detailed evaluation of the proposed algorithm in a larger data base and the characterization of the detected network in order to discriminate typical from atypical patterns which are important cues to detect malign lesions.

ACKNOWLEDGMENT

We thank Profs. Teresa Mendonça, André Marçal and Ms. Barbara Amorim from the University of Porto, Drs. Ofelia Morais, Marta Pereira, Marta Teixeira and nurse Lina Santos from Hospital Pedro Hispano, for their support during this work.

REFERENCES

[1] Dermoscopy Tutorial, www.dermoscopy.org/atlas/base.htm

[2] J. Mayer, Systematic review of the diagnostic accuracy of dermatoscopy in detecting malignant melanoma, Medical Journal Australia, 206-210, 1997.

[3] H. Pehamberger, A. Steiner, K. Wolff, In vivo epiluminescence microscopy of pigmented skin lesions. I. Pattern analysis of pigmented skin lesions. Journal of American Academy of Dermatololy, vol. 17, 571-583 1987

[4] Scott W. Menzies, A Method for the diagnosis of primary cutaneous melanoma using surface microscopy, Dermatologic Clinics Vol. 19, 299-305, 2001.

[5] W. Stolz et al., ABCD rule of Dermatoscopy: a new practical method for early recognition of malignant melanoma, European Journal of Dermatology, vol. 4, 521-527, 1994.

[6] G. Argenziano et al., Epiluminescence microscopy for the diagnosis of doubtful melanocytic skin lesions. Comparison of the ABCD rule of dermatoscopy and a new 7-point checklist based on pattern analysis, Archive of Dermatology, vol. 134, 1563-1570, 1998.

[7] P. Rubegni et al., Automated diagnosis of pigmented skin lesions, International Journal of Cancer, Vol. 101, 576-580, 2002.

[8] H. Iyatomi, et al., An Improved Internet-Based Melanoma Screening System with Dermatologist-like Tumor Area Extraction Algorithm, Computerized Medical Imaging and Graphics, Vol. 32. 566-579, 2008.

[9] N. Situ et al., Malignant Melanoma Detection by Bag-of-Features Classication, 3110-3113, EMBS 2008.

[10] R. Duda, P. Hart, D. Stork, Pattern Classification, Wiley, 2001.

[11] G. Betta, et al., Dermoscopic image-analysis system: estimation of atypical pigment network and atypical vascular pattern, IEEE International Workshop on Medical Measurement and Applications. 63-67, 2006.

[12] M. E. Celebi, H. Iyatomi, W. V. Stoecker, R. H. Moss, H. S. Rabinovitz, G. Argenziano, H. P. Soyer, Automatic Detection of Blue-White Veil and Related Structures in Dermoscopy Images, Computerized Medical, Vol. 32. 670-677, 2008.

[13] G. Fabbrocini et al., Epiluminescence Image Processing for Melanocytic Skin Lesion Diagnosis Based on 7-Point Check-List, Open Dermatology Journal, 110-115, 2010.

[14] M. Sadeghi, M. Razmara, M. Ester, T. K. Lee, M. S. Atkins, Graph-based Pigment Network Detection in Skin Images, Proc. SPIE 7623, 2010.

[15] N. Situ, X. Yuan, G. Zouridakis, Assisting Main Task Learning by Heterogeneous Auxiliary Tasks with Applications to Skin Cancer Screening, International conference on artificial intelligence and statistics, April 2011.

[16] M. Bertalmio, G. Sapiro, V. Caselles, C. Ballester, Image Inpainting, SIGGRAPH, 417-424, 2000.